A Kinetic Model of Dihydrolipoamide Dehydrogenase from Multiple Organisms

Michael A. Moxley [1], Jason N. Bazil [2], and Daniel A. Beard[2]

[1]Department of Biochemistry, Medical College of Wisconsin, [2]Department of Molecular and Integrated Physiology, University of Michigan

Abstract

Dihydrolipoamide dehydrogenase is a flavoenzyme that catalyzes the oxidation of dihydrolipoamide to lipoamide with the concomitant reduction of NAD^+ to NADH. *In vivo* this enzyme is a subunit of the pyruvate, α-ketoglutarate, and glycine dehydrogenase complexes where it catalyzes the final reaction in a sequence of oxidative reactions. Of these, the pyruvate dehydrogenase complex is a well-known regulator of central metabolism located in mitochondria and its activity is dependent on many factors including intracellular NAD^+/NADH ratio which are sensed directly through the lipoamide dehydrogenase component.

It has been established that dihydrolipoamide dehydrogenase becomes inactivated when catalyzing the reverse reaction in the absence of added NAD^+ and that this inactivation is more prominent at low pH. The proposed mechanism behind the inactivation is an overly reduced four electron dead-end state that is traditionally shown to occur by excess NADH to NAD^+ ratio. Here we analyze a host of kinetic datasets from human, rat, spinach, and *E. coli*, showing that all datasets can be fitted to a common kinetic mechanism that accounts for this unique pH and NAD^+ dependent activation/inhibitory phenomenon.

The kinetic mechanism that we have identified is rapid and random in the binding and dissociation of substrates and products and accounts for the possibility of either ternary or ping-pong type pathways. Overall, our mechanism reproduces observations of NAD^+ dependent progress curve lags, pH and NAD^+ dependent velocity profile shifts, and product inhibition patterns while maintaining equilibrium and thermodynamic cycle constraints.

Overall Dihydrolipoamide Dehydrogenase reaction

$$Dihydrolipoamide + NAD^+ \rightleftharpoons Lipoamide + NADH + H^+$$

Proposed Kinetic Model of Dihydrolipoamide Dehydrogenase

Figure 1. A) A four state mechanism with rapid equilibrium binding of substrates and products where E_1, E_2, E_3, and E_4 represent the oxidized, two electron reduced charge transfer intermediate, hydride reduced FAD, and four electron reduced dead-end state, respectively. In panel A, dihydrolipoamide, NAD^+, lipoamide, NADH, and a proton are represented by A, B, P, Q, and H^+ respectively. The fraction of each enzyme state bound to substrate or product is represented by *f* where a subscripted letter indicates the chemical species that is bound and subscripted numbers indicate the enzyme state. B) The mechanism shown in panel A was simplified to three states so that the two electron reduced states (E_2 and E_3 in panel A) have been grouped into one state (now E_2), according to previous observations that this step occurs very quickly. C) Substrates and products are considered to bind randomly and in rapid equilibrium to each major state indicated by equilibrium dissociation constants of the corresponding substrates. D) Proton binding sites on the thiolate and active site base, typically a histidine residue, are modelled to further dictate whether certain substrate or product bound species can execute a chemical step in the mechanism.

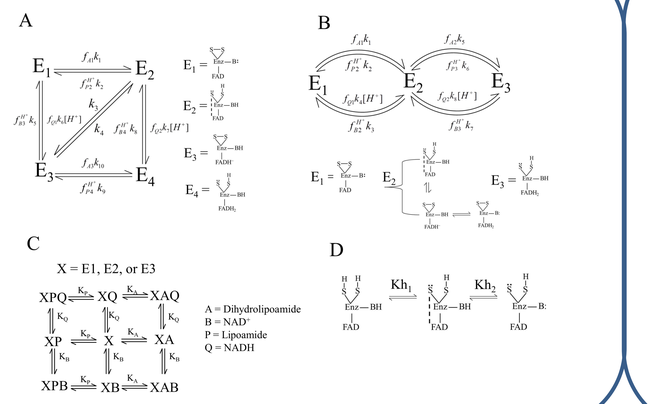

Model Solution and Expressions

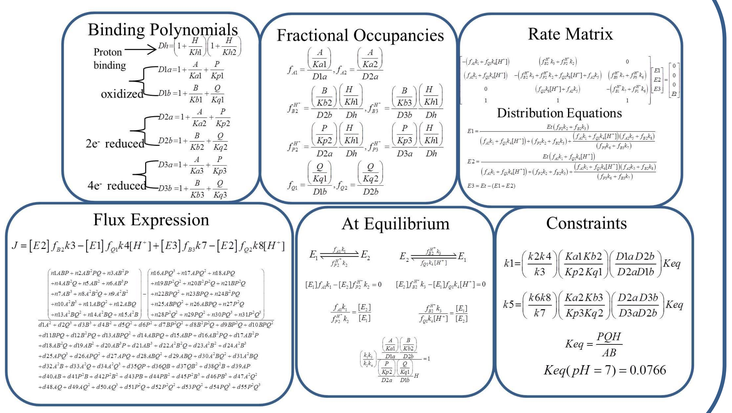

Rat Liver Enzyme Fitting

Data from JBC vol. 248 pp.4834-39 (1973)

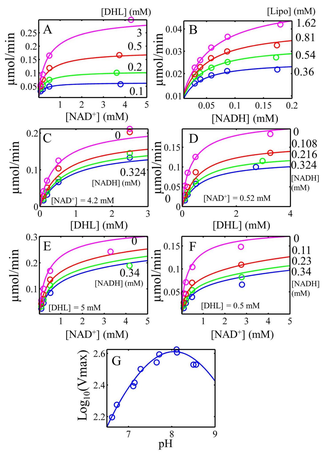

Figure 2. A-B) Initial velocity data collected in the absence of products where (A) and (B) are in the forward and reverse direction respectively. C-F) Product inhibition initial velocity data . G) Log_{10}(Vmax) of the forward reaction with pH.

E.coli Enzyme Fitting

Data from
JBC vol. 256 pp.2307-14 (1981)
JBC vol. 264 pp.8039-45 (1989)

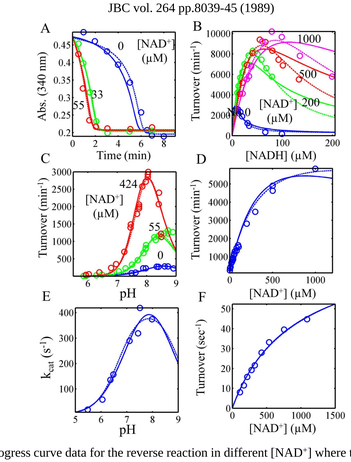

Figure 3. A) Progress curve data for the reverse reaction in different $[NAD^+]$ where the solid line is from a fit with a single Kd set and the dotted line is from a multiple Kd set so that the Kd depends on the oxidation state of the enzyme. B) Reverse reaction varying NADH with different $[NAD^+]$. C) Initial velocity as a function pH and $[NAD^+]$. D) Activation of reverse initial velocity with $[NAD^+]$.E) k_{cat} as a function of pH. F) Turnover number as a function of $[NAD^+]$.

Spinach Enzyme Fitting

Data from
JBC vol. 238 pp.1869-76 (1963)

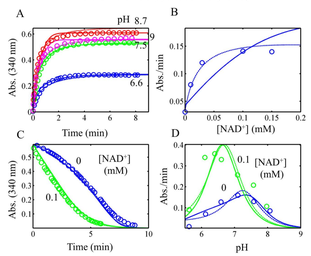

Figure 4. A) Progress curve data for the forward reaction with varied pH where the solid line is from a fit with a single Kd set and the dotted line is from a multiple Kd set so that the Kd depends on the oxidation state of the enzyme. B) Activation of reverse initial velocity with $[NAD^+]$. C) Progress curve data for the reverse reaction in different $[NAD^+]$. C) Initial velocity of the reverse reaction as a function of pH and $[NAD^+]$.

Human Liver Enzyme Fitting

Data from
JBC vol. 242 pp.54-60 (1967)

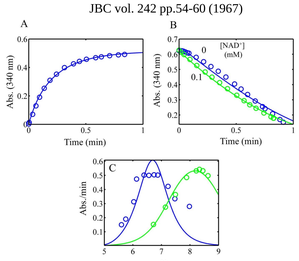

Figure 5. A) Progress curve data for the forward reaction (pH = 8.5). B) Progress curve data for the reverse reaction in different $[NAD^+]$ (pH = 6.5). C) Initial velocity as a function of pH for the forward (green) and reverse reaction (blue).

Enzyme Species Distributions

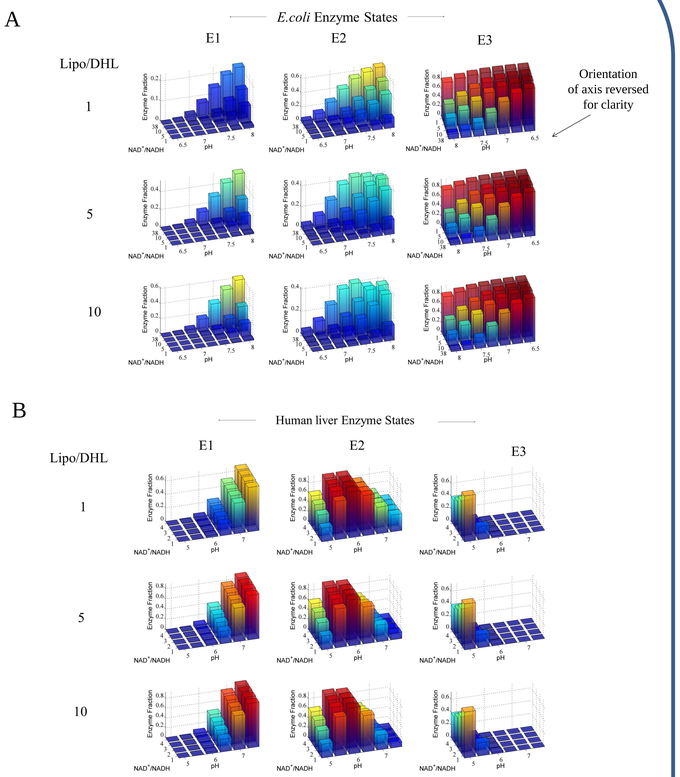

Figure 6. Enzyme species distributions calculated from best fit parameters and lipoamide/dihydrolipoamide (Lipo/DHL) and NAD^+/NADH ratios as a function of pH. A) *E. coli* enzyme species distributions calculated from best fit parameters from a single Kd set model. NAD^+/NADH ratios were chosen based on literature data collected in aerobic conditions (Cited below). B) Human liver enzyme species distributions calculated from best fit parameters from a single Kd set model. NAD^+/NADH ratios in an approximate range of literature estimations were used. Lipo/DHL ratios were arbitrarily chosen. The total concentrations of nicotinamide and lipoyl reactants were held constant at 3 mM and 10 mM respectively. (Journal of Bacteriology vol. 181 p. 2351-57 (1999))

Kinetic Parameters

	Rat liver cit/γ/mc		Human liver cit/γ/mc		*E. coli* cit/γ/mc			Spinach cit/γ/mc	
Parameter	**Single K_d set**	**Sensitivity**	**Single K_d set**	**Sensitivity**	**Single K_d set**	**Multiple K_d set**	**Sensitivity**	**Single K_d set**	**Multiple K_d set**	**Sensitivity**
$^a k_f$ (min^{-1})	**4.08×10^4**	–	**4.83×10^5**	–	**5.56×10^6**	–	–	**2.78×10^7**	–	–
k_2 (min^{-1})	980	0.167	**1.01×10^5**	0.349	**1.2×10^5**	**5.46×10^4**	0.582 (0.556[b])	**3.17×10^6**	**1.95×10^5**	0.308 (1.04)
k_3 (min^{-1})	**8.38 x 10^4**	**0.0844**	**9.87 x 10^5**	**0.202**	**2.62 x 10^6**	**5.95 x 10^4**	**0.0695 (0.138)**	**10^5**	**10^6**	**0.184 (0.135)**
k_4 (min^{-1})	10^7	0.118	**2.08×10^6**	0.171	**8.42×10^6**	10^7	0.151 (0.206)	**6.33×10^7**	**5.86×10^7**	0.255 (0.294)
$^a k_b$ (min^{-1})	**1.23 x 10^4**	–	**2.18×10^5**	–	**1.18×10^6**	–	–	**3.42×10^5**	–	–
k_6 (min^{-1})	**1.85 x 10^7**	0.490	10^7	**8.42×10^{-4}**	70.1	357	0.133 (0.157)	10^5	**1.47×10^5**	0.670 (0.128)
k_7 (min^{-1})	**4.32 x 10^5**	**0.239**	**1.18 x 10^6**	**0.0210**	**8.58 x 10^4**	**3.67 x 10^4**	**0.456 (0.394)**	**2.60 x 10^6**	**3.85 x 10^5**	**0.520 (0.901)**
k_8 (min^{-1})	**8.20 x 10^7**	0.340	**1.14 x 10^8**	0.0213	10^7	10^7	0.430 (0.419)	**6.43 x 10^6**	**5.0 x 10^4**	0.487 (0.950)
pKh1	**8.05**	**0.215**	**9**	**0.0342**	**8.62**	**8.71**	**0.192 (0.160)**	**9**	**8.9**	**0.030 (0.017)**
pKh2	8.05	0.246	7.32	0.366	7.12	7.0	0.282 (0.245)	5.67	4	0.297 (0.01)
K_{s1} (nM)	**924**	**0.280**	**581**	**0.0037**	**10^4**	**174**	**6.33 x 10^4 (5.7 x 10^{-4})**	**155**	**4.88**	**0.040 (6.4 x 10^{-6})**
K_{iB} (μM)	1.70 x 10^3	0.352	4.0	0.0904	**1.19 x 10^3**	**4.54 x 10^3**	0.429 (0.025)	2.70	2.55	0.361 (0.163)
K_{P1} (nM)	**758**	**0.600**	**34**	**0.0345**	**1**	**45.8**	**0.0171 (9.1 x 10^{-5})**	**3.26**	**33.3**	**0.0393 (6.4 x 10^{-6})**
K_{iQ} (nM)	1.22 x 10^3	0.447	3.2	0.0906	3.19 x 10^3	4.77 x 10^3	0.408 (0.241)	3.55	1	0.338 (0.166)
K_{s2} (nM)	–	–	–	–	–	**10^4**	**8.84 x 10^4**	–	**5.05 x 10^3**	**0.0105**
K_{iA} (μM)	–	–	–	–	–	1.02 x 10^3	0.095	–	26.2	0.0701
K_{P2} (nM)	–	–	–	–	–	**2.04 x 10^3**	**0.327**	–	**19.6**	**0.0320**
K_{iQ} (nM)	–	–	–	–	–	1.46 x 10^3	0.399	–	1	0.0654
K_{s3} (nM)	–	–	–	–	–	1	**0.0203**	–	1	**0.0610**
K_{iA} (μM)	–	–	–	–	–	43	0.305	–	26.6	0.380
K_{P3} (nM)	–	–	–	–	–	**2.88 x 10^3**	**0.120**	–	**10^4**	**0.111**
K_{iQ} (μM)						7.88	0.307	–	10^4	0.0028
K_{eq} (pH =7)	**0.206**	**0.655**	**0.106**	**0.0528**	**0.039**	**0.153**	**0.0836 (0.129)**	**0.0383**	**0.0446**	**0.302 (0.115)**

[a]Parameter was solved for based on thermodynamic cycle constraint
[b]Sensitivities in parenthesis correspond with multiple Kd fits

Summary

- Datasets of dihydrolipoamide dehydrogenase from multiple organisms have illustrated the importance of the NAD^+/NADH ratio and pH in the activation/inhibition of this enzyme
- Here we, for the first time, globally fit datasets from a number of organisms to a model that explains the unique kinetic behavior of dihydrolipoamide dehydrogenase in numerous conditions including pH dependency
- The model we have identified allows for random binding at both the lipoyl and nicotinamide binding sites, inactivation due to protonation state of the active site base and thiolate, and accounts for thermodynamic cycle and equilibrium constraints
- Our results show that a three state mechanism can be used to describe all of the datasets which include initial velocity and product inhibition data, as well as both pH and NAD dependent progress curve data in both directions that includes a lag in certain conditions
- This model can be further used as a kinetic regulatory component of complexes that use this enzyme such as the PDH complex

Funding

This research has been supported by NIH T32: HL094273 and R01: DK095210